# Magnetically induced transition in the spectrum of Sr IV

M. C. Li,[1] K. Wang,[2] T. Brage,[3] and R. Hutton[4,*]

[1]*School of Electronic Information and Electrical Engineering, Huizhou University, Huizhou, 516007, China*

[2]*Hebei Key Lab of Optic-electronic Information and Materials, The College of Physics Science and Technology, Hebei University, Baoding, 071002, China*

[3]*Division of Mathmatical Physics, Department of Physics, Lund University, 22100 Lund, Sweden*

[4]*Shanghai EBIT Laboratory, Institute of Modern Physics, Fudan University, Shanghai, 200433, China and Key Laboratory of Nuclear Physics and Ion-beam Application (MOE), Fudan University, Shanghai, 200433, China*

(Received 21 December 2020; accepted 9 March 2021; published 31 March 2021)

Observations and studies of what we call magnetic induced transitions have arguably re-opened a whole new area of atomic spectroscopy. There are transitions from upper levels that are sensitive to externally applied magnetic fields, such as those in tokamaks and the solar corona. So far only two types of ionic systems have been confirmed as leading to magnetic induced transitions, namely Ne-like Ar and Fe, and Cl-like Fe. We here propose a homologous system to Cl-like ions, namely Br-like ions, as a new candidate. These transitions are fed by close degeneracy between levels of relative short and long lifetimes, respectively. A similar close degeneracy as in Cl-like Fe is present in Br-like Sr and will give rise to an observable magnetic induced transition. We have predicted the magnetic induced transition rate for the $^4D_{7/2}$ level in Sr IV as a function of magnetic field strengths.

DOI: 10.1103/PhysRevA.103.032831

## I. INTRODUCTION

In 2003 an unexpected line was observed in a spectrum of Ne-like Ar IX recorded at the Electron Beam Ion Trap, EBIT, at the Lawrence Livermore National Laboratory [1]. The line came from the $2p^5 3s\,^3P_0 \rightarrow 2p^6\,^1S_0$ transition, which is forbidden for single-photon decay in the absence of external field, for this element with a nucleus with zero spin. The energy levels of $Ar^{8+}$ were well enough known to confirm that this line was indeed what is now labeled a magnetic induced transition, MIT [2]. This discovery opened up an novel way to diagnose the magnetic field of plasma. It was shown in Ref. [1] that a magnetic field, of around 1.1 and 3 T, used in the EBIT to compress the electron beam was enough to mix the $^3P_0$ level with the $^3P_1$ and $^1P_1$ levels and induce the $2p^5 3s\,^3P_0 \rightarrow 2p^6\,^1S_0$ MIT transition as an E1 decay. This transition requires on the order of a few Tesla to be observable even in a low density plasma. The combination of requiring a high magnetic field and low density plasma meant it was not really plausible to see this line in naturally occurring or fusion plasmas. Therefore research on MITs did not really gain momentum until 2015 when an MIT in the spectrum of Cl-like iron, Fe X, was discovered [3,4]. This discovery led to the first spectral determination of the field in the solar corona, with a method that could be used in continuously monitoring its active regions [5]. In this paper we continue the search for other MITs, in other ionic systems and report on one candidate in the Br-like sequence. This sequence with the ground states of $4s^2 4p^5$ is homologous to the Cl-like sequence, with a ground state of $3p^5$.

## II. STRUCTURE OF BR-LIKE IONS AND POSSIBLE MIT IN SR IV

In Fig. 1 we show the energy structure of the lowest seven levels of Br-like ions with $Z$ between 36 and 40. The two levels of interest for this current paper are the $^4D_{7/2}$ and $^4D_{5/2}$ of the $4s^2 4p^4 4d$ configuration. Both of these can decay to the $^2P_{3/2}$ level of the $4s^2 4p^5$ ground configuration by what we call expected transitions [2,6]. The $^4D_{7/2}$ state, in the absence of an external magnetic field or nuclear spin, can only decay to the ground state through a forbidden magnetic quadrupole (M2) transition with a rate of the order of several $s^{-1}$, which is six orders of magnitude smaller than the electric dipole (E1) transition rate of the $^4D_{5/2}$ state. In the presence of an external magnetic field, the magnetic interaction introduces a mixing between these two $^4D$ states, opening up a magnetic induced electric dipole transition (MIT-E1) to the ground state. This MIT-E1 transition rate, to first order, is given by [3]

$$A_{\mathrm{MIT}} \propto \frac{B^2}{\Delta \mathrm{E}^2} A_{E1}, \tag{1}$$

where B is the external magnetic field strength, $\Delta$E is the energy difference between the $^4D_{5/2}$ and $^4D_{7/2}$ states and $A_{E1}$ is the transition rate of the $^4D_{5/2}$ state. For most of the Br-like ions the energy difference $\Delta$E is too large to give rise to an observable MIT in any magnetic field of interest. But, by chance the $^4D_{7/2}$ level crosses the $^4D_{5/2}$ level between strontium and yttrium leading to a minimum fine structure energy (see Fig 2). Figure 2 shows the energy difference $\Delta$E of Br-like ions from Kr II to Zr VI. It is clear that the fine structure splitting energy of Sr IV is the smallest splitting among the five ions leading to a an enhanced MIT-E1 transition decay channel of the $^4D_{7/2}$ level for this ion.

*rhutton@fudan.edu.cn

 ©2021 American Physical Society

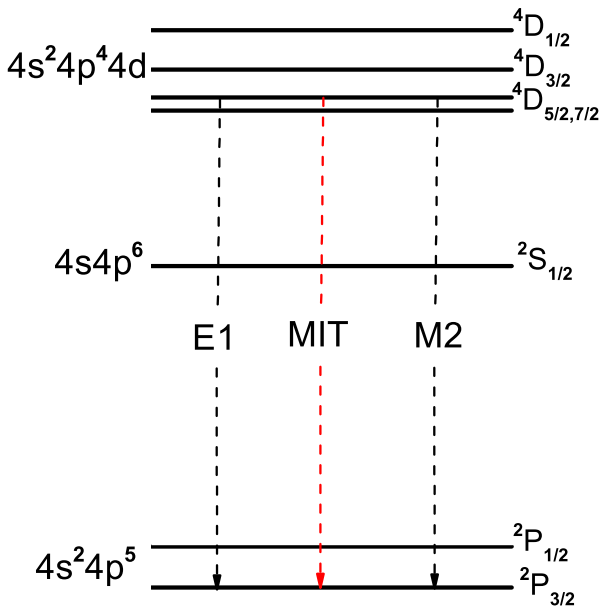


FIG. 1. Schematic energy level diagram of Br-like ions with Z between 36 and 40. Note that the $^4D_{7/2}$ is the lowest level of the $4s^24p^44d$ configuration for $Z \leqslant 38$, while it will change to the second lowest level when $Z > 38$.

## III. THEORETICAL METHOD

### A. The MCDHF method

The fully relativistic multiconfiguration Dirac-Hartree-Fock (MCDHF) method [7] implemented in the GRASP2K package [8] is adopted in the present work. In this, the atomic state functionS were expressed as a linear combination of configuration state functions (CSFs), $\Phi(\gamma_i J)$

$$\Psi(\gamma J) = \sum_i c_i \Phi(\gamma_i J). \tag{2}$$

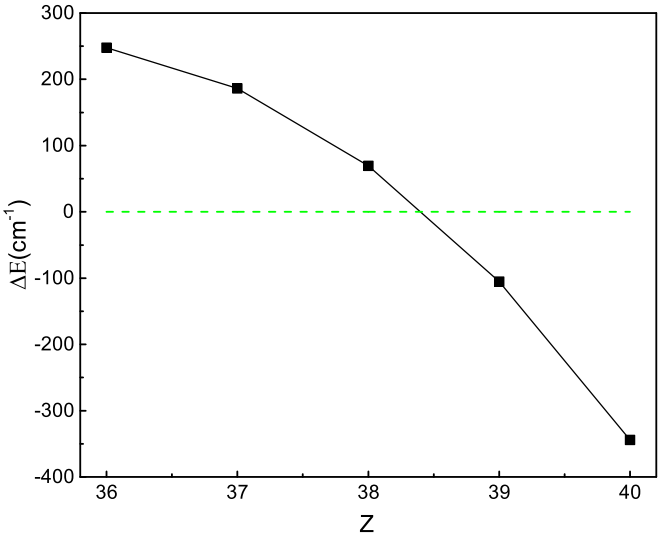


FIG. 2. Fine-structure energies, ΔE, for $4s^24p^44d\,^4D_{7/2,5/2}$ of Br-like ions from present calculation. The dashed line in green represent ΔE = 0.

TABLE I. Summary of the number of levels in the reference set and CSFs in the total expansion for each J and parity of the blocks in the final step of MCDHF calculations.

| J | Parity | # Levels | # CSFs |
|---|---|---|---|
| 1/2 | − | 1 | 416184 |
| 3/2 | − | 1 | 762953 |
| 1/2 | + | 1–6 | 150567 |
| 3/2 | + | 1–8 | 332047 |
| 5/2 | + | 1–8 | 452679 |
| 7/2 | + | 1–5 | 438666 |
| 9/2 | + | 1–2 | 232816 |

The CSFs are antisymmetrized linear combination of products of single-electron Dirac orbitals. Through relativistic self-consistent field procedure, the single-electron Dirac orbitals and the expansion coefficients $c_i$ are all optimized to self-consistency. Then the frequency-independent Breit interaction and the leading part of the quantum electrodynamic (QED) effects (self energy and vacuum polarization) are taken into account in the subsequent relativistic configuration interaction (RCI) calculations [8,9].

In the MCDHF calculations, the even and odd atomic states are determined separately by using the extended optimal level [10] scheme. We started with a Dirac-Hartree-Fock (DHF) calculation including only the CSF from the multireference set and with no excitation allowed from it. The multireference set included configurations
$4s^24p^5$, $4s4p^54d$, $4s^24p^34d^2$, $4s^24p^44f$
for the odd states and
$4s4p^6$, $4s^24p^44d$, $4s^24p^34d4f$, $4s4p^44d^2$, $4s^24p^24d^3$, $4s4p^54f$, $4p^64d$, $4s^24p^24d4f^2$
for the even states.

Subsequently, the CSFs expansions are obtained through single and double excitation from shells occupied in the first two configurations in the multireference to an active set of orbitals. In the active set the maximum one electron quantum numbers, $n_{\max}l_{\max}$, are $n_{\max} \leqslant 7$ and $l_{\max} \leqslant 4$ for excitations from the $n = 4$ shell, and $n_{\max} \leqslant 6$ and $l_{\max} \leqslant 3$ for excitations from the $3d$ and $3p$ subshells. We define the $n = 4$ shell as containing the valence electrons, while the other shells represent the core of the ions. Based on this definition, the valence-valence and core-valence correlation effects are both included in the calculations. The total number of configurations in the final step of core-valence calculation for each of the blocks defined by parity ($P$) and total angular momentum ($J$) are summarized in Table I. In the following RCI calculation, the final CSFs expansions for the different J symmetries is the same as final step of core-valence calculation.

### B. Magnetic induced transition (MIT)

An example of unexpected transitions [2,6] that has recently attracted attention, are induced by the interaction between an external and static magnetic field and an atom/ion with zero nuclear spin. These are usually referred to as magnetic induced transitions (MITs). The details of magnetic interaction theory can be found in Refs. [11,12], but was already outlined in the textbook by Cowan (see section 17.6

TABLE II. $M$-dependent magnetic induced $|7/2, M\rangle \rightarrow |3/2, M'\rangle$ transition rates $A_{\rm MIT}(M)$ (in $s^{-1}$) at the magnetic field strengths $B = 1$T for Br-like isotopes of ions between Kr II and Zr VI without nuclear spin. The rates for the $-1/2$ to $1/2$ and the $-M$ to $-M'$ transitions are similar to their counterparts. $x[n]$ implies $x10^n$.

| | $A_{\rm MIT}(M)$ | | | | |
|---|---|---|---|---|---|
| $M \rightarrow M'$ | $Kr^{+}$ | $Rb^{2+}$ | $Sr^{3+}$ | $Y^{4+}$ | $Zr^{5+}$ |
| $5/2 \rightarrow 3/2$ | 7.22[0] | 2.01[1] | 3.86[2] | 5.09[1] | 2.05[1] |
| $3/2 \rightarrow 3/2$ | 4.60[0] | 1.28[1] | 2.56[2] | 3.31[1] | 1.17[1] |
| $3/2 \rightarrow 1/2$ | 7.22[0] | 2.01[1] | 3.85[2] | 5.09[1] | 2.05[1] |
| $1/2 \rightarrow 3/2$ | 1.44[0] | 4.02[0] | 7.69[1] | 1.02[1] | 4.10[0] |
| $1/2 \rightarrow 1/2$ | 8.28[0] | 2.31[1] | 4.60[2] | 5.95[1] | 2.10[1] |
| $1/2 \rightarrow -1/2$ | 4.33[0] | 1.21[1] | 2.31[2] | 3.06[1] | 1.23[1] |

in Ref. [13]). In the present discussion on Br-like ions we will focus on the two lowest states $^4D_{7/2,5/2}$ of the second excited configuration $4s^24p^44d$, here labeled as $|7/2, M\rangle$ and $|5/2, M\rangle$, which will mix with each other in the presence of an external magnetic field. Here $M$ is the magnetic quantum number of the levels. The final mixed state $|\text{“}7/2\text{”}, M\rangle$ can be expressed as

$$|\text{“}7/2\text{”}, M\rangle \approx d_0(M)|7/2, M\rangle + d_1(M)|5/2, M\rangle, \quad (3)$$

where $d_1(M)$ will be referred to as the mixing coefficients of the two levels. It is, to first order, given by

$$d_1(M) = -B\sqrt{\frac{49-4M^2}{63}}\frac{\langle {}^4D_{5/2} \parallel \mathbf{N}^{(1)} + \Delta\mathbf{N}^{(1)} \parallel {}^4D_{7/2}\rangle}{\mathrm{E}(^4\mathrm{D}_{7/2}) - \mathrm{E}(^4\mathrm{D}_{5/2})}, \quad (4)$$

where $\mathbf{N}^{(1)}$ is the tensor operator and $\Delta\mathbf{N}^{(1)}$ is the Schwinger QED correction [14].

According to the selection rules for different transitions, the $|5/2, M\rangle$, but not the $|7/2, M\rangle$, has an expected E1 transition to the ground state $4s^24p^5\,{}^2P_{3/2}$ labeled as $|3/2, M'\rangle$. The $|\text{“}7/2\text{”}, M\rangle$, however, gets an induced decay channel to the $|3/2, M'\rangle$ through a magnetic field induced E1 transition (MIT-E1). The MIT-E1 transition rate from specific $M$ sublevels in $|\text{“}7/2\text{”}, M\rangle$ to $|3/2, M'\rangle$ can be written as

$$\begin{aligned} &A_{\rm MIT}(M, M')(\text{“}7/2\text{”}, M \rightarrow 3/2, M') \\ &\quad \approx |d_1(M)|^2 A(5/2, M \rightarrow 3/2, M') \\ &\quad \approx a^R_{\rm MIT}(M, M')\frac{B^2}{\lambda^3(\Delta\mathrm{E})^2}, \end{aligned} \quad (5)$$

where $\Delta\mathrm{E} = \mathrm{E}(^4D_{5/2}) - \mathrm{E}(^4D_{7/2})$ is the fine structure splitting energy and $a^R_{\rm MIT}$ is the reduced transition rate

$$a^R_{\rm MIT}(M, M') = \frac{32\pi^3(49-4M^2)}{189\hbar}\sum_{q=-1}^{1}\left|\begin{pmatrix} 3/2 & 1 & 5/2 \\ -M' & q & M \end{pmatrix}\langle {}^4D_{5/2}\|\mathbf{N}^{(1)} + \Delta\mathbf{N}^{(1)}\|{}^4D_{7/2}\rangle\langle {}^2P_{3/2}\|\mathbf{P}^{(1)}\|{}^4D_{5/2}\rangle\right|^2 \quad (6)$$

The E1 $|5/2, M\rangle \rightarrow |3/2, M'\rangle$ transition matrix elements and the magnetic interaction matrix elements can be obtained by using the RTRANSITION and updated HFSZEEMAN modules [12] included in the GRASP2K package.

## IV. RESULTS AND DISCUSSION

### A. Br-like ions from Kr II to Zr VI

As mentioned in Sec. III B, the radiative E1 decay channel from the $4s^24p^44d\,{}^4D_{7/2}$ with $M\epsilon\{\pm5/2, \pm3/2, \pm1/2\}$ will be induced by an external magnetic field. The magnetic induced $|\text{“}7/2\text{”}, M\rangle \rightarrow |3/2, M'\rangle$ E1 transition rates are dependent on the magnetic quantum number $M$ of the sublevels belonging to the $4s^24p^44d\,{}^4D_{7/2}$ according to Eqs. (3) and (4). The magnetically induced E1 transition rates from each magnetic sublevel in $4s^24p^44d\,{}^4D_{7/2}$ to the magnetic sublevels of $4s^24p^5\,{}^2P_{3/2}$ for a magnetic field of $B = 1$T are shown in Table II. As we can see in Table II, Sr IV has the largest magnetic induced rates for all magnetic sublevels.

To give a more transparent representation and to compare with the magnetic quadrupole (M2) decay rate, we list the magnetic induced transition rates $\bar{A}_{\rm MIT}$ averaged over the magnetic sublevels, as a sum over $M$ and $M'$;

$$\bar{A}_{\rm MIT} = \frac{\sum_{M,M'} A_{\rm MIT}(M, M')}{2\mathrm{J}+1}. \quad (7)$$

Based on Eq. (7), we give the average of the magnetic induced transition rates $\bar{A}_{\rm MIT}$ for magnetic field strengths of 0.5, 1, 1.5, and 2 T in Table III, together with the M2 transition rates $A_{M2}$ and the fine structure energy $\Delta$E. Experimental fine structure energies were used in the calculation of the magnetic induced transition rates $\bar{A}_{\rm MIT}$. For the calculation of the rate of the $^4D_{5/2} \rightarrow {}^2P_{3/2}$ transition, labeled as $A_{E1}$ in Eq. (1), we use the length gauge formulation. This is considered to be more accurate than the corresponding velocity gauge formulation. This also leads us to some idea on the uncertainty of the $A_{E1}$ rate. We can estimate this uncertainty from $\delta T = |T_{\rm length} - T_{\rm velocity}|/\max(T_{\rm length}, T_{\rm velocity})$ [15] where T is a transition probablity. We find an uncertainly of 10%.

The decay of the $4s^24p^44d\,{}^4D_{7/2}$ state to the ground state $4s^24p^5{}^2P_{3/2}$ is dominated by the magnetic quadrupole (M2) transition in the absence of an external magnetic field.

TABLE III. Average magnetic induced transition rates, $\bar{A}_{\rm MIT}$ (in $s^{-1}$) at different magnetic field strengths ($B$) (in T), together with the M2 transition rates, $A_{M2}$ (in $s^{-1}$) and the fine structure splitting energy $\Delta$E (in $cm^{-1}$) for Br-like Kr II to Zr VI. $x[n]$ implies $x10^n$ except for the column labeled experiment. Note that the $\Delta$E used to calculate the $\bar{A}_{\rm MIT}$ are the experimental values.

| | | | $\bar{A}_{\rm MIT}$ | | | | $\Delta$E | |
|---|---|---|---|---|---|---|---|---|
| Z | Ions | $A_{M2}$ | B = 2 | B = 1.5 | B = 1 | B = 0.5 | Experiment | Calculation |
| 36 | $Kr^{+}$ | 1.72[0] | 2.97[1] | 1.76[1] | 8.96[0] | 3.77[0] | 217.06 [16] | 247.78 |
| 37 | $Rb^{2+}$ | 4.17[0] | 8.30[1] | 4.88[1] | 2.44[1] | 9.80[0] | 156.00 [17] | 186.11 |
| 38 | $Sr^{3+}$ | 8.83[0] | 1.78[3] | 1.00[3] | 4.51[2] | 1.19[2] | 40.41 [18] | 69.33 |
| 39 | $Y^{4+}$ | 1.60[1] | 2.25[2] | 1.32[2] | 6.52[1] | 2.52[1] | −139.67 [19] | −105.36 |
| 40 | $Zr^{5+}$ | 2.62[1] | 6.43[1] | 4.71[1] | 3.49[1] | 2.75[1] | −382.78 [20] | −344.26 |

However, the unexpected MIT-E1 transition channel will open if an external magnetic field exists. From Eq. (5), it is clear that the MIT-E1 rate is strongly dependent on the fine structure splitting energy, in addition to the strength of the magnetic field. The $\Delta E$ varies along the isoelectronic sequence, with a clear minimum for Sr IV (see Fig. 2). In Fig 3 we plot the rates for the $4s^24p^44d\,^4D_{7/2} \rightarrow 4s^24p^5\,^2P_{3/2}$ transition, $A = \bar{A}_{\rm MIT} + A_{M2}$, for different magnetic field strengths, B, along the Br-like sequence. Figure 3 illustrates the strength of the enhancement for Sr IV ($Z = 38$) ion of the MIT-E1 transition.

### B. Sr IV

We focus on the interesting case of Sr IV with the strong MIT-E1 rate due to the close degeneracy between the $^4D_{7/2}$ and $^4D_{5/2}$ levels. In this section we discuss how the intensity of the MIT-E1 line from the $^4D_{7/2}$ level in Sr IV varies with the magnetic field. For clarity, we discussed the rate for this line normalized to the expected E1 line from the $^4D_{5/2}$ which does not depend on the magnetic field.

We present simulations of the line ratio as a function of magnetic field for electron densities $\rho_e = 1 \times 10^{11}\,{\rm cm}^{-3}$ in Fig 4. Note that an electron density must be chosen for the modeling as the $^4D_{7/2}$ level transition rate is quite low, even when including the MIT, so the level will be density sensitive. As can be seen from Fig. 4 the intensity ratio of the unexpected MIT $4s^24p^44d\,^4D_{7/2} \rightarrow 4s^24p^5\,^2P_{3/2}$ transition to the $4s^24p^44d\,^4D_{5/2} \rightarrow 4s^24p^5\,^2P_{3/2}$ is a monotonic function of the magnetic field strength. The simulation was based on the collisional-Rradiative modeling in the flexible atomic code (FAC_ [21]. The configurations $3p^63d^{10}4s^24p^5$, $3p^63d^{10}4s4p^6$, $3p^63d^{10}4s^24p^4[4[d,f]$, $3p^63d^{10}4s^24p^34d4f$, $3p^63d^{10}4s^24p^4nl$, $3p^63d^{10}4s4p^5nl$, $3p^63d^94s^24p^5[4[d,f]$, $3p^53d^{10}4s^24p^54[d,f]$, $3p^63d^94s^24p^6$, $3p^53d^{10}4s^24p^6$, $3p^63d^94s^24p^55l'$, $3p^53d^{10}4s^24p^55l'$ with $5 \leqslant n \leqslant 7$, $l \leqslant n-1$ and $l' \leqslant 4$ were included in the present simulation. There are 2264 levels included in the present simulation and all the radiative transition rates (E1,E2,E3,M1,M2,M3) have been included. The level energies and radiative transition rates were calculated by the fully relativistic configuration interaction method implemented in the FAC.

## V. CONCLUSIONS

We have discussed a magnetic induced transition in the spectrum of Sr IV. This transition is homologous to the earlier investigated MIT in Fe $X$ [3,5], and originates through a

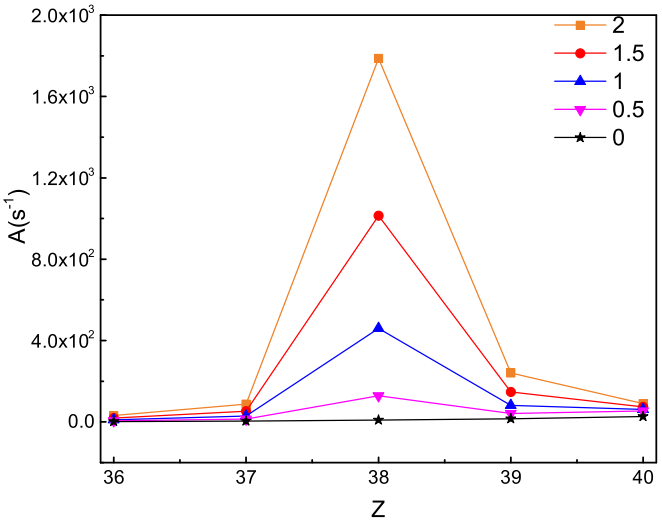


FIG. 3. The total $4s^24p^44d\,^4D_{7/2} \rightarrow 4s^24p^5\,^2P_{3/2}$ transition rates $A = \bar{A}_{\rm MIT} + A_{M2}$ for different magnetic field strengths B for Br-like ions from Kr II to Zr VI.

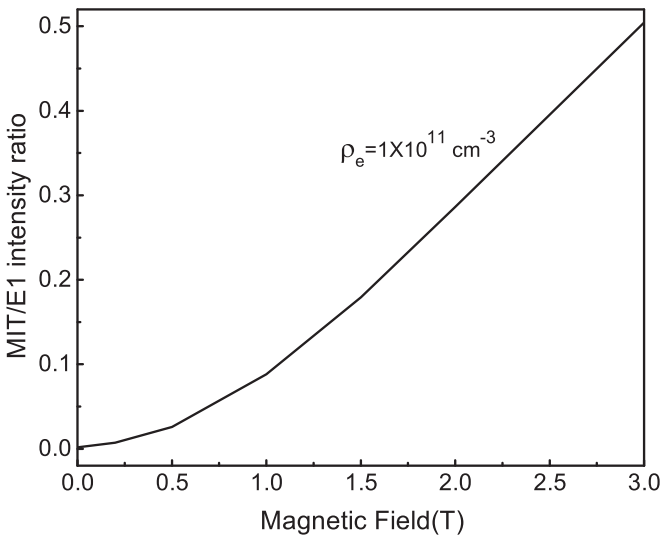


FIG. 4. The simulated line ratio of $4s^24p^44d\,^4D_{7/2} \rightarrow 4s^24p^5\,^2P_{3/2}$ (MIT) and $4s^24p^44d\,^4D_{5/2} \rightarrow 4s^24p^5\,^2P_{3/2}$ (E1 transition) of Sr IV as a function of magnetic field strength B for an electron density of $\rho_e = 1 \times 10^{11}\,{\rm cm}^{-3}$. The electron energy distribution used in this simulation was a 45 eV Maxwellian.

mixing of the $^4D_{5/2}$, which has an allowed transition to the ground $^2P_{3/2}$ level, and the metastable $^4D_{7/2}$. It could be argued that, to the best of our knowledge, this is only the third ionic system with an observable MIT that has been carefully investigated. We encourage further explorations to find more candidates of MIT. The basic requirements for two energy levels to give rise to these are: as near degenerate in energy as possible, not differing by more than one in angular momentum quantum number, the same parity and one level should have an allowed, i.e., relatively fast decay, whereas the other level should be metastable.

## ACKNOWLEDGMENTS

This work was supported by The Professorial and Doctoral Scientific Research Foundation of Huizhou University No. 158020137.

[1] P. Beiersdorfer, J. H. Scofield, and A. L. Osterheld, Phys. Rev. Lett. **90**, 235003 (2003).
[2] J. Grumer, T. Brage, M. Andersson, J. G. Li, P. Jönsson, W. X. Li, Y. Yang, R. Hutton, and Y. M. Zou, Phys. Scr. **89**, 114002 (2014).
[3] W. X. Li, J. Grumer, Y. Yang, T. Brage, K. Yao, C. Y. Chen, T. Watanabe, P. Jönsson, H. Lundstedt, R. Hutton, and Y. M. Zou, Astrophys. J. **807**, 69 (2015).
[4] W. X. Li, Y. Yang, B. S. Tu, J. Xiao, J. Grumer, T. Brage, T. Watanabe, R. Hutton, and Y. M. Zou, Astrophys. J. **826**, 219 (2016).
[5] R. Si, T. Brage, W. X. Li, J. Grumer, M. C. Li, and R. Hutton, Astrophys. J. **898**, L34 (2020).
[6] T. Brage, M. Andersson, and R. Hutton, AIP Conf. Proc. **1125**, 18 (2009).
[7] C. F. Fischer, M. Godefroid, T. Brage, P. Jönsson, and G. Gaigalas, J. Phys. B **49**, 182004 (2016).
[8] P. Jönsson, G. Gaigalas, J. Bieroń, C. F. Fischer, and I. P. Grant, Comput. Phys. Commun. **184**, 2197 (2013).
[9] I. P. Grant, B. J. McKenzie, P. H. Norrington, D. F. Mayers, and N. C. Pyper, Comput. Phys. Commun. **21**, 207 (1980).
[10] K. G. Dyall, I. P. Grant, C. T. Johnson, F. A. Parpia, and E. P. Plummer, Comput. Phys. Commun. **55**, 425 (1989).
[11] M. Andersson and P. Jönsson, Comput. Phys. Commun. **178**, 156 (2008).
[12] W. X. Li, J. Grumer, T. Brage, and P. Jönsson, Comput. Phys. Commun. **253**, 107211 (2020).
[13] R. D. Cowan, *The Theory of Atomic Structure and Spectra* (University of California Press, Berkeley, CA, 1981).
[14] K. T. Cheng and W. J. Childs, Phys. Rev. A **31**, 2775 (1985).
[15] C. F. Fischer, Phys. Scr. **T134**, 014019 (2009).
[16] E. B. Saloman, J. Phys. Chem. Ref. Data **36**, 215 (2007).
[17] J. E. Sansonetti, J. Phys. Chem. Ref. Data **35**, 301 (2006).
[18] T. Rauch, P. Quinet, M. Knörzer, D. Hoyer, K. Werner, J. W. Kruk, and M. Demleitner, Astrom. Astrophys. **606**, A105 (2017).
[19] J. Reader, Atoms **4**, 31 (2016).
[20] J. Reader and M. D. Lindsay, Phys. Scr. **91**, 025401 (2016).
[21] M. F. Gu, Canadian J. Phys. **86**, 675 (2008).